PNNL-12048
UC-2000

Pacific Northwest
National Laboratory
Operated by Battelle for the
U.S. Department of Energy

Uranium Mobility During In Situ Redox Manipulation of the 100 Areas of the Hanford Site

J. E. Szecsody
K. M. Krupka
M. D. Williams
K. J. Cantrell
C. T. Resch
J. S. Fruchter

November 1998

Prepared for the U.S. Department of Energy
under Contract DE-AC06-76RLO 1830

DISCLAIMER

PACIFIC NORTHWEST NATIONAL LABORATORY
operated by
BATTELLE
for the
UNITED STATES DEPARTMENT OF ENERGY
under Contract DE-AC06-76RLO 1830

Printed in the United States of America

Available to DOE and DOE contractors from the Office of Scientific and Technical Information, P.O. Box 62, Oak Ridge, TN 37831; prices available from (615) 576-8401.

Available to the public from the National Technical Information Service, U.S. Department of Commerce, 5285 Port Royal Rd., Springfield, VA 22161

PNNL-12048
UC-2000

Uranium Mobility During In Situ Redox Manipulation of the 100 Areas of the Hanford Site

J. E. Szecsody
K. J. Cantrell
K. M. Krupka
C. T. Resch
M. D. Williams
J. S. Fruchter

November 1998

Prepared for
the U.S. Department of Energy
under Contract DE-AC06-76RLO 1830

Pacific Northwest National Laboratory
Richland, Washington 99352

Summary

A series of laboratory experiments and computer simulations was conducted to assess the extent of uranium remobilization that is likely to occur at the end of the life cycle of an in situ sediment reduction process. The process is being tested for subsurface remediation of chromate- and chlorinated solvent-contaminated sediments at the Hanford Site in southeastern Washington. Uranium species that occur naturally in the +6 valence state [U(VI)] at 10 ppb in groundwater at Hanford will accumulate as U(IV) through the reduction and subsequent precipitation conditions of the permeable barrier created by in situ redox manipulation. The precipitated uranium will be remobilized when the reductive capacity of the barrier is exhausted and the sediment is oxidized by the groundwater containing dissolved oxygen and other oxidants such as chromate. Although U(IV) accumulates from years or decades of reduction/precipitation within the reduced zone, U(VI) concentrations in solution are only somewhat elevated during aquifer oxidation because oxidation and dissolution reactions that release U(IV) precipitate to solution are slow. The release rate of uranium into solution was found to be controlled mainly by the oxidation/dissolution rate of the U(IV) precipitate (half-life 200 hours) and partially by the fast oxidation of adsorbed Fe(II) (half-life 5 hours) and the slow oxidation of $Fe(II)CO_3$ (half-life 120 hours) in the reduced sediment. Simulations of uranium transport that incorporated these and other reactions under site-relevant conditions indicated that 35 ppb U(VI) is the maximum concentration likely to result from mobilization of the precipitated U(IV) species. Experiments also indicated that increasing the contact time between the U(IV) precipitates and the reduced sediment, which is likely to occur in the field, results in a slower U(IV) oxidation rate, which, in turn, would lower the maximum concentration of mobilized U(VI). A six-month-long column experiment confirmed that uranium accumulated in reduced sediment was released slowly into solution with U(VI) concentrations at only slightly greater than influent U(VI) concentrations. This experiment also demonstrated that dissolved chromate, another oxidant likely to be present in some field systems, did not increase the release rate of uranium into solution.

Acknowledgments

This work was prepared with the support of the following contributors:

DOE Headquarters	Office of Science and Technology Grover Chamberlain
Focus Area/Program	Subsurface Contaminant Focus Area James Wright
Operations Office	Richland Operations Office Science and Technology Programs Division Deborah E. Trader, Technical Program Officer
Contractor	Pacific Northwest National Laboratory Environmental Science and Technology Environmental Technology Division Rod K. Quinn, Manager

PLEASE BE AWARE THAT
ALL OF THE MISSING PAGES IN THIS DOCUMENT
WERE ORIGINALLY BLANK

Contents

Figures

1.0 Introduction

This report describes a limited set of laboratory experiments and computer simulations that were used to assess the potential of uranium mobility associated with the in situ redox manipulation process that is being considered for use for remediation of chromate-contaminated sediment at the 100 areas of the U.S. Department of Energy's Hanford Site (Fruchter et al. 1996, 1997). The proposed remediation technology introduces a reductant (sodium dithionite buffered at high pH) for a short time into the contaminated sediment to reduce Fe(III) oxides present in the sediment to aqueous or surface-bound Fe(II) (Amonette et al. 1994). The reduced Fe(II) appears to be present in several different phases: adsorbed Fe(II), structural Fe(II), and Fe(II)-carbonate (siderite) and is referred to as "reduced sediment" in this report. Uranium species naturally occurring in the +6 valence state [U(VI)] at 10 ppb in groundwater at the Hanford Site in southeastern Washington will accumulate to U(IV) through the eduction and subsequent precipitation conditions of the permeable redox barrier (Figure 1). Small-scale batch experiments were conducted to quantify the rate of U(VI) reduction and precipitation in the reduced sediment.

The focus of this study is to quantify the rate and extent of uranium release to solution that occurs during the end of the life cycle of the redox barrier. The precipitated uranium will be remobilized when the reductive capacity of the barrier is exhausted and the sediment oxidized by the groundwater containing dissolved oxygen and other oxidants such as chromate. In this research, the rate of uranium remobilization during the oxidation of sediment was addressed in batch systems under a variety of field-relevant conditions. The reaction rate and extent of uranium immobilization in the reduced sediment and mobilization as the sediment is oxidized were quantified using a multireaction, multisolute code. Reaction parameters were then used to simulate the reactive transport of uranium species under a variety of conditions. A six-month-long column experiment was conducted to confirm the validity of predictions in a small 1-D homogeneous transport system in which uranium was accumulated for considerable time in the reduced sediment, then mobilized as the sediment was oxidized. Additional transport simulations (1- and 2-D) were conducted to simulate other field-relevant scenarios and incorporate other processes such as spatial heterogeneities to predict the expected peak concentrations of mobilized uranium.

This report briefly reviews uranium mobility concepts as they pertain to this redox barrier (Section 2), followed by a description of the laboratory experiments and simulations. These results are presented according to the following sequential life-cycle phases of the redox barrier: a) uranium mobility in oxic groundwater, (Section 3) b) uranium immobilization under reducing conditions (Section 4), c) uranium remobilization reactions (Section 5), and d) uranium remobilization during reactive transport (Section 6). Our conclusions are presented in Section 7, and cited references can be found in Section 8. The appendix contains supporting information on the analysis of uranium.

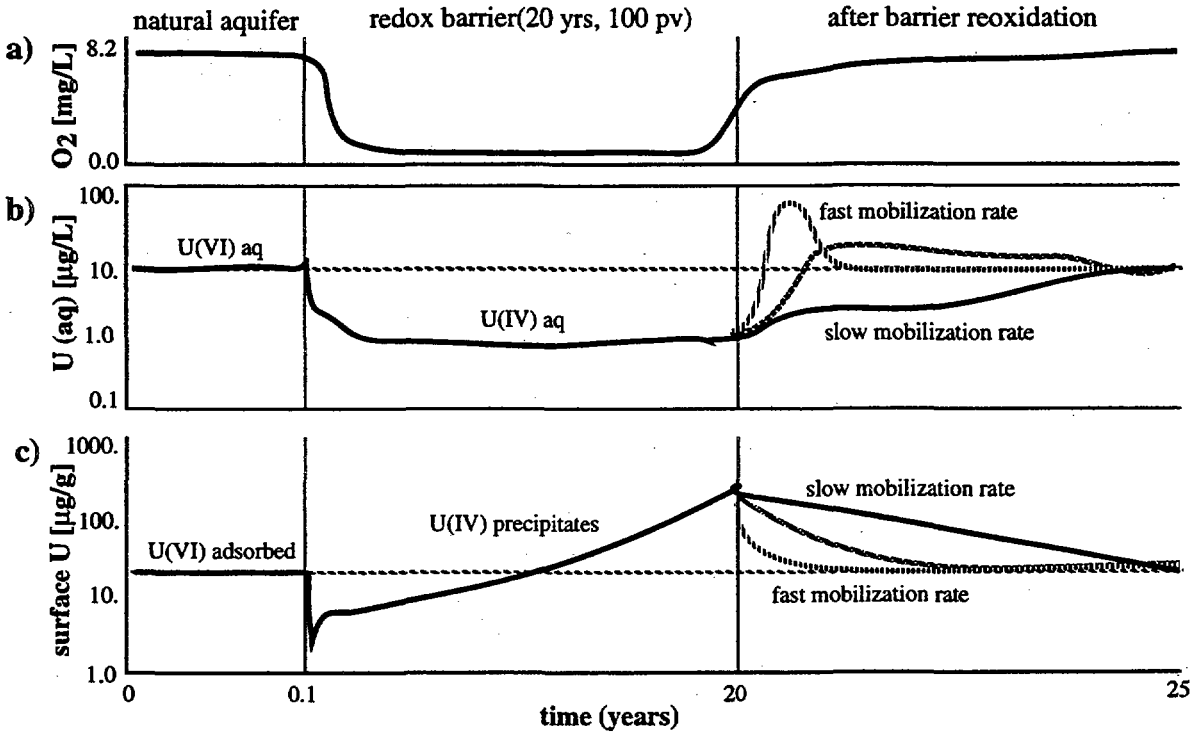

Figure 1. Conceptual Diagram Showing the Influence of a Redox Barrier as a Function of Time on a) the redox conditions of groundwater (dissolved oxygen shown), b) the concentration of aqueous uranium species, and c) the concentration of surface uranium species that result from adsorption or precipitation

2.0 Uranium Mobility Concepts

Naturally occurring uranium is present in the 100 H area of the Hanford Site at a concentration of about 9.5 ± 4.4 ppb (parts per billion or $\mu g\ L^{-1}$) as measured in seven wells in 1996–97 in the unconfined aquifer (pH 7.7, near oxygen-saturated conditions) (Fruchter et al. 1996). The concentrations of dissolved uranium at this pH under oxidizing conditions are controlled by the aqueous speciation of U(VI) and adsorption of U(VI) species onto sediments. The transport of uranium species through aquifer sediments varies considerably with geochemical conditions such as pH and oxidation/reduction (redox). Under the reduced conditions (oxidation-reduction potential [Eh] <0.0 V) present in the redox barrier, the dissolved U(VI) species are reduced to the less-soluble U(IV), and precipitate. However, these accumulated U(IV) solids will be remobilized into solution when the redox barrier is oxidized at the end of its life cycle. The mass of accumulated uranium and the rate at which the redox barrier and U(IV) precipitate oxidize control the resulting peak concentration of dissolved uranium.

2.1 Uranium Speciation and Transport in Oxic Aquifer Conditions

We know a lot about the speciation of uranium in the +3, +4, +5, and +6 oxidation states in aqueous environments (Langmuir 1978; Wanner and Forest 1992). Dissolved U(III) easily oxidizes to U(IV) under most redox conditions found in nature. The U(V) aqueous species (UO_2^+) readily disproportionates to U(IV) and U(VI); consequently, U(IV) and U(VI) are the most common oxidation states of uranium in nature. Uranium is generally found in the +6 oxidation state in oxidizing environments and in the +4 oxidation state in reducing environments.

Dissolved U(VI) readily hydrolyzes to form several aqueous complexes. In carbonate-free systems, important species include UO_2^{2+}, $UO_2(OH)_2^0(aq)$, $UO_2(OH)_3^-$, $(UO_2)_3(OH)_5^+$, and $(UO_2)_2(OH)_2^{2+}$ (Wanner and Forest 1992). The concentrations of these species and their distribution relative to other U(VI) species is a function of pH and the total concentration of dissolved U(VI). A large number of other important U(VI) species exist in more chemically complex aqueous systems; for example, in the unconfined aquifer of the Hanford 100 areas, at pH 7.7 in predominately carbonate-containing water and oxidizing conditions, major species present are carbonate anions [60% $UO_2(CO_3)_3^{4-}$, 30% $UO_2(CO_3)_2^{2-}$, 10% $(UO_2)_3(OH)_5^+$](Langmuir 1978). This speciation changes with pH and Eh (redox condition), but the conditions remain relatively constant in the natural aquifer. In this report, this distribution of species is referred to as "U(VI) aqueous species." Organic complexes are also generally important to aqueous uranium speciation, but the unconfined aquifer of the Hanford Site contains very little natural organic matter.

Given the concentration of uranium that is naturally present in the Hanford 100-Area sediments, adsorption of U(VI) to specific mineral phases of the sediments is the primary control on uranium mobility at pH 7.7 under oxidizing conditions. At higher concentrations, the solubility of U(VI)-containing minerals could control the maximum concentrations of dissolved uranium in the sediments. Uranium minerals that can form in oxic conditions and control the concentration of dissolved uranium include carnotite [$(K_2(UO_2)_2(VO_4)_2]$, schoepite ($UO_3 \cdot 2H_2O$), rutherfordine (UO_2CO_3), tyuyamunite [$Ca(UO_2)_2(VO_4)_2$], autunite [$Ca(UO_2)_2(PO_4)_2$], potassium autunite [$K_2(UO_2)_2(PO_4)_2$], and uranophane [$Ca(UO_2)_2(SiO_3OH)_2$] (Frondel 1958; Langmuir 1978).

Aqueous U(VI) species interact with Hanford area sediments even under oxidizing conditions. At the concentrations of dissolved uranium naturally present in the unconfined aquifer and the higher solubility of dissolved U(VI) relative to that of U(IV), adsorption reactions will be the primary control on uranium mobility in oxic conditions and at this pH (Figure 1, 0 to 0.1 year). An accurate prediction of adsorption involves determining the partitioning of each U(VI) aqueous specie between solution and each solid phase (amorphous and crystalline minerals, natural organic matter). Measurement of individual species adsorption to separate solid phases over a pH range (i.e., pH adsorption edges) can then be combined with other experimental information about the solid phases and modeled to determine thermodynamic constants for the solid phases (i.e., acidity constants) and adsorbing species (i.e., adsorption constants). If this type of measurement were possible for the three to six major U(VI) species over a pH range [60% $UO_2(CO_3)_3^{4-}$, 30% $UO_2(CO_3)_2^{2-}$, 10% $(UO_2)_3(OH)_5^{+}$ at pH 7.7] to at least four solid phases [amorphous iron oxide, goethite, magnetite, clays], then a total partitioning of mass between the aqueous and solid phases could be rigorously developed for specific geochemical conditions (pH, Eh, and ionic strength). However, direct measurement of the various U(VI)-carbonate species is not analytically possible, and substantial resources would be needed to determine the adsorption characteristics of measurable species to the different solid phases.

A second approach was taken to provide a reasonable estimate of the partitioning of mass between aqueous and solid phases. This development of a partition or distribution coefficient (K_d) is applicable to a small range of geochemical conditions that exist in the natural (unaltered) aquifer because the pH and redox conditions change little. Measuring the distribution coefficient is highly useful for this study because it can be used to describe the overall transport and attenuation of uranium species. The simplest type of distribution coefficient considers only the amount of mass in solution and on the solid phases at equilibrium:

$$\text{U(VI) (aq)} \; <==> \; \text{U(VI) adsorbed} \qquad (1)$$

where the number of adsorption sites are considerably greater than the adsorbed mass, and so are assumed not to change. This "linear" adsorption approach is used to define a distribution coefficient and, in transport systems, a retardation factor:

$$K_d = [\text{U(VI)aq}] / [\equiv \text{U(VI)}] \qquad (2)$$

$$R_f = 1 + \rho_b K_d / \theta \qquad (3)$$

where $[U(VI)_{aq}]$ is the aqueous uranium concentration ($\mu g\ cm^{-3}$), $[\equiv U(VI)]$ is the surface adsorbed uranium concentration ($\mu g\ g^{-1}$), R_f is the retardation factor defined as the relative velocity of U(VI) species to water, ρ_b is the dry bulk density ($g\ cm^{-3}$), and θ is the porosity. With no adsorption ($K_d = 0.0\ cm^3\ g^{-1}$), uranium moves at the speed of groundwater, but with progressively greater adsorption uranium moves more slowly, because proportionally greater mass is on the surface (or, alternatively, uranium species spend proportionally more time on the surface). This linear adsorption approach is applicable only over a small range of U(VI) concentrations over which adsorption energy is constant (adsorption of a single species could be assumed) as is the number of sites (valid at a low $U(VI)_{aq}$ concentration). Considering only the additional effect of the number of surface sites (pH and redox conditions are still considered constant):

$$U(VI)\,(aq) + \equiv \quad <==> \quad \equiv U(VI) \tag{4}$$

where ≡ is a surface site that can be used to define Langmuir adsorption:

$$[\equiv U(VI)] = MK_L[U(VI)aq] / [1 + K_L[U(VI)aq]] \tag{5}$$

where M is the total number of surface sites (or site concentration, μmol/g), and K_L is the Langmuir affinity parameter ($cm^3/\mu mol$). This Langmuir model assumes a single type of adsorption site, which may be valid for a natural sediment if a single phase dominates the adsorption. At very small concentrations, adsorption is linear and $MK_L \approx K_d$, whereas at high concentration, adsorption decrease is eventually limited by the total number of sites. At these higher concentrations, K_d is a function of the aqueous uranium concentration:

$$K_d' = [\equiv U(VI)] / [U(VI)aq] = MK_L[U(VI)aq] / [1 + K_L[U(VI)aq]] /[U(VI)aq] \tag{6}$$

With this concentration-dependent K_d', the retardation factor can still be defined (3) to determine the relative velocity of uranium through the aquifer.

Whereas a pure adsorbent has a single type of adsorption site with constant affinity and typically is fit well with a Langmuir isotherm, natural sediments can contain several mineral phases that adsorb the solute of interest. The sum of adsorption to these different phases (i.e., addition of several Langmuir isotherms from each mineral phase) provides an overall adsorption isotherm for the sediment. If mineral phases that have less surface area have higher affinities, the resulting overall isotherm will have a slope less than 1.0 at low concentration. In the absence of determining the U(VI) adsorption isotherms of each mineral phase in the sediment, an empirical isotherm (Langmuir-Freundlich) can be used to fit isotherm data with nonlinear slopes at low concentration:

$$K_d'' = [\equiv U(VI)] / [U(VI)aq] = M[K_{LF}U(VI)aq]^b / [1 + [K_{LF}U(VI)aq]^b] /[U(VI)aq] \tag{7}$$

The deviation of the slope (from 1.0) at low concentration provides an indication of the influence of multiple adsorption sites that have differing affinities. For U(VI) species adsorption, a non-linear slope may also be caused by the presence of multiple U(VI) species that are adsorbing. Reactive transport of uranium species defined by this concentration-dependent isotherm is also defined by the retardation factor (3).

2.2 Uranium Speciation and Transport in Reducing Aquifer Conditions

Under the reducing conditions (Eh < 0.0 V) in the dithionite-reduced sediment, the dissolved U(VI) species normally present in oxic water (shown conceptually in Figure 1 at 0 to 0.1 year) are reduced to the less soluble +4 valence state resulting in precipitation of sparingly soluble U(IV) species or mixed U(IV)/U(VI) solids. The total concentration of dissolved U(IV) species in reducing groundwater is quite low because of the low solubility of U(IV) solid phases (Bruno et al. 1988, 1991). The aqueous speciation of dissolved U(IV) at pH >3 is dominated by hydrolytic species such as $U(OH)_3^+$ and $U(OH)_4^0(aq)$. U(IV) complexes with chloride, fluoride, phosphate,

and sulfate are unimportant above pH 3, but a recent study indicates that U(IV)-carbonate complexes might be significant at higher concentrations of dissolved carbonate (Rai et al. 1990).

Reduction of U(VI) to U(IV) usually results in the precipitation of U(IV) (e.g., uraninite, compositions ranging from UO_2 to $UO_{2.25}$) or mixed U(IV)/U(VI) solids (e.g., U_4O_9). In this report, these U(IV) solids are referred to as U(IV) precipitates. Other important U(IV) minerals found in nature include coffinite ($USiO_4$) and ningyoite ($CaU(PO_4)_2{\cdot}2H_2O$) (Langmuir 1978; Frondel 1958). Thus, as groundwater containing U(VI) aqueous species is transported through the permeable reduced zone, there will be an accumulation of U(IV) precipitates (Figure 1, 0.1 to 20 years). The processes that define this accumulation are 1) the combined rate of U(VI) reduction and U(IV) precipitation and 2) the capacity of the reduced iron [Fe(II)] barrier.

The immobilization of the aqueous uranium species as it contacts the redox barrier has conceptual similarities to the formation of uranium roll-front deposits in sandstone rocks, and some insight is gained from those studies. These ore bodies occur when U(VI) carried by oxic groundwater contacts a zone containing a naturally occurring reductant such as natural organic matter and $H_2S(g)$ (Adler 1974; Maynard 1983). The U(VI) is reduced to U(V) at this interface and U(IV)-containing minerals that form as precipitates include uraninite and coffinite.

2.3 Barrier Oxidation and Uranium Remobilization

The accumulated U(IV) precipitate will be remobilized into solution when the reduced iron barrier is oxidized (Figure 1, after 20 years). The rate at which this mass of U(IV) is remobilized controls the resulting concentration of dissolved U(VI) species, which may or may not result in an initial concentration peak (Figure 1b). Several processes affect this rate, including 1) the U(IV) precipitate oxidation rate, 2) the Fe(II) oxidation rate, 3) U(IV) precipitate-sediment aging, 4) U(VI) solubility limits, and 5) sediment chemical and physical heterogeneities. Quantitative determination of the rates or effects of these processes is needed to accurately predict the uranium concentration that can result as the reduced iron barrier is oxidized. If the combination of these processes results in fast uranium solubilization, the dissolved U(VI) concentrations can peak at a value higher than the natural 9.5 ppb. Alternatively, if these processes result in slow uranium solubilization, then the U(VI) concentration will increase slowly to natural levels (Figure 1b).

The oxidation of the adsorbed and structural Fe(II) in the sediments of the permeable redox barrier occurs naturally by the inflow of dissolved oxygen through the barrier, but it can be oxidized by contaminants that may be present, such as chromate, as well. As described below, the oxidation rate of the reduced iron barrier is controlled by a combination of several chemical oxidation reactions and possibly physical (diffusion) limitations in accessing sites. Using dissolved oxygen as an oxidant can occur via two electron sequences:

$$O_2 + 2H^+ + 2e^- \Longleftrightarrow H_2O_2 \quad (8)$$

$$H_2O_2 + 2H^+ + 2e^- \Longleftrightarrow H_2O \quad (9)$$

so 4 moles of electrons are available per mole of O_2 consumed. The second reaction (9) is much slower than the first, although with many transition metals such as Fe(II) the reaction kinetics can be described with a single first-order reaction (Stumm and Morgan 1981). Oxidation of structural and adsorbed Fe(II) by several mechanisms, including

$$Fe^{3+} + e^- \leftrightarrows Fe^{2+} \quad (10)$$

$$Fe(OH)_3(s) + 3H^+ + e^- \leftrightarrows Fe^{2+} + 3H_2O \quad (11)$$

$$Fe(OH)_3(s) + 2H^+ \; HCO_3^- + e^- \leftrightarrows FeCO_3(s) + 3H_2O \quad (12)$$

generally indicates that 1 mole of electrons is consumed per mole of Fe(II) oxidized. Experimental evidence indicates that the oxygenation of Fe(II) in solutions (pH >5) is generally found to be first order with respect to Fe(II) and O_2 concentration and second order with respect to OH-. Therefore, approximately 4 moles of Fe(II) are oxidized per mole of O_2 consumed (reactions 8–10), and the rate increases one-hundred-fold for a unit increase in pH. At oxygen-saturated conditions (8.2 ppm O_2), 1.02 mmol L^{-1} Fe(II) is consumed.

Chromate present as a contaminant in groundwater will also oxidize Fe(II)

$$HCrO_4^- + 7H^+ + e^- \leftrightarrows Cr^{3+} + 4H_2O \quad (13)$$

with 1 mole of electrons consumed per mole of chromate reduced. The reduction of one mole of chromate oxidizes one mole of Fe(II) [reactions 10 and 13], or mg L^{-1} chromate is needed to oxidize the equivalent mass of Fe(II) as water saturated with dissolved oxygen [1.02 mmol L^{-1} Fe(II)]. Chromate is considered a much stronger oxidizer than dissolved oxygen, so even at concentrations less than mg L^{-1} it may influence the iron oxidation rate.

Similar geochemical reactions that are important for mobilization of U(VI) during the reduced iron barrier oxidation also occur during alkaline in situ leach mining of uranium deposits, although the chemistries of oxidizing solutions are significantly different. Most current uranium recovery operations use various alkaline leaching techniques including ammonia carbonate-bicarbonate solutions and an oxidant (IAEA 1980, 1993). For in situ mining, oxygen is not considered effective for oxidation of UO_2 at practical rates under ambient pressure and temperature. The U(VI)-carbonate species formed are similar to those described in the natural carbonate waters in this report, but the concentrations used in the mining operations are considerably higher. Also, the carbonate leaching operations typically involve elevated pressure and temperature to increase the dissolution. Thus, based on these comparisons and the results from the experiments and computer modeling simulations described in this report, we propose that the peak uranium concentrations resulting from the "natural" oxidation of the redox barrier will be significantly lower than what would be obtained if in situ uranium mining techniques were used on the same sediments.

The oxidation rate of the redox barrier is controlled by the rate at which dissolved oxygen in water flowing through the sediment oxidizes the different forms of Fe(II), so it is a combination of several chemical oxidation rates and possibly physical (i.e., diffusion) limitations in accessing sites. The U(IV) precipitates on sediments slowly recrystallize over time so are likely to be more recalcitrant over decades of precipitate contact with the reduced sediments. Processes such as intraparticle diffusion, coprecipitation, and overgrowth of other precipitates or oxides also reduce the ability of the sediment to release uranium into solution quickly under the eventual oxic conditions. Such processes have been reported for uranium precipitates on sediments (Payne et al. 1994). Even under optimal conditions for U(IV) oxidation, the total concentration of uranium will also be limited by the aqueous solubility limit under the specific geochemical conditions. As the sediment is slowly oxidized (i.e., the Eh increases from -0.6 V to +0.4 V), the uranium solubility slowly increases. The combination of physical heterogeneities (i.e., higher permeability zones) and

chemical heterogeneities [zones of differing Fe(II) mass and speciation] will result in portions of the reduced barrier being oxidized before other portions. This will result in the release of uranium to solution over a longer period of time than with a completely homogeneous sediment.

2.4 Reaction and Reactive Transport Modeling

In this study, numerical modeling was used to simulate both batch and column systems with one or multiple reactions. Differential forward and reverse mass flux equations of the species for the reactions considered in each case (Szecsody et al. 1994, 1998b) were solved numerically with the fourth-order Runge-Kutta method in batch and a stiff reaction solver method during transport (Hindmarsh 1983). The accuracy of the batch reaction model and submodel of the transport code RAFT (Chilakapati 1995) was tested by comparing it with analytical solutions of a single first-order reaction, a mixed first-second-order reaction, and two reactions (series and parallel).

The chemical reaction submodel was readily incorporated into the transport code with an operator splitting technique to solve the reactive contributions from advection and dispersion separately. Three-dimensional advective transport was solved by a modified method of characteristics in which incompressible flow was obtained by the characteristic-conservative method and the concentrations were obtained by the characteristic-mixed method (Arbogast et al. 1992). The combined method is a direct numerical approximation of the Reynolds transport theorem in that fluid packets are followed along volume-preserving streamlines and the dispersive, reactive contributions are computed. The code has been tested extensively and the convergence of the numerical methods established (Chilakapati et al. 1998). The accuracy of the multireaction reactive transport system in this study was compared with an analytical solution of transport with a single kinetic reaction (Parker and van Genuchten 1984) and a numerical code transport with multiple kinetic/equilibrium reactions (Salvage et al. 1995; Yeh et al. 1998).

3.0 Uranium Transport in Natural (oxic) Aquifer Conditions

3.1 Batch Adsorption Experiments

Dissolved U(VI) species interact with Hanford Area sediments even under oxidizing conditions. At the concentrations of dissolved uranium naturally present in the unconfined aquifer at the Hanford 100 H Area (~10 ppb), uranium adsorption to sediments was investigated. Oxygen-saturated conditions were used as a high Eh endpoint, although the conditions in the aquifer vary from 3 to 8 mg/L. Two batch experiments were considered to develop a general estimate of the partitioning of U(VI) species between the aqueous phase and various mineral surfaces of the sediment. These experiments consisted of mixing 0.01 to 3.0 g of Hanford 100 H sediment with 5 to 20 mL of synthetic groundwater containing 10 to 1000 ppb uranium for 48 hours, then analyzing the uranium remaining in solution. The sediment was from well H5-8 at 44 to 45 ft, and the <4.7-mm fraction was used in the experiments. The synthetic groundwater consists of deionized water and salts to create a solution of the major ions found in the unconfined aquifer (15 mg/L NaCl, 8.2 mg/L KCl, 67 mg/L $CaSO_4$, 13 mg/L $MgCO_3$, 150 mg/L $CaCO_3$, and 15.3 mg/L H_2SiO_3), and the pH was adjusted to 7.7–8.6.

The adsorption isotherm experiment considers adsorption over a range of uranium concentrations with the pH and Eh fixed. As described in Section 2.1, a linear correlation between the mass adsorbed and in solution indicates a large number of adsorption sites, and the partitioning can be modeled as a single species adsorbing to a single type of site. Decreasing adsorption at higher concentrations would indicate a limited number of sites. A nonlinear slope at low concentrations indicates more than one major type of adsorption affinity (i.e., several mineral phases and/or several aqueous species). The pH edge experiment consists of measuring adsorption at different pH values while keeping the Eh and uranium concentration fixed. This type of experiment can be used to determine whether the multiple U(VI)-carbonate solution species present are reacting as anions. Buffers to maintain pH were not used in any of these uranium experiments due to complexation with uranium. Instead, the pH was carefully checked and adjusted over several hours or days using HCl or NaOH.

Analysis of both surface and solution species confirmed that aqueous species and surface species oxidation state. One filtered liquid sample (no additional treatment) was used to measure U(VI) species in solution (Brina and Miller 1992, 1993, Appendix), and a second filtered liquid sample was treated with 0.03% peroxide to oxidize any U(IV) to U(VI). The difference between the total solution uranium in this liquid sample [$U(VI)_{aq} + U(IV)_{aq}$] and the previous [$U(VI)_{aq}$] in solution gave $U(IV)_{aq}$. The sediment containing any adsorbed or reduced/precipitated uranium species was washed and treated with 2 mol L^{-1} HNO_3 to mobilize uranium species (which should not oxidize uranium). Analysis of this sample provided $U(VI)_{surface}$ (i.e., [$U(VI)_{aq} + U(VI)_{surface}$] - [$U(VI)_{aq}$]). A second sample of this solubilized surface uranium was then treated with 0.03% peroxide to oxidize any surface U(IV) to U(VI) to quantify $U(IV)_{surface}$ (i.e., [$U(VI)_{surface} + U(IV)_{surface} + U(VI)_{aq} + U(IV)_{aq}$] - [$U(VI)_{aq} + U(IV)_{aq}$] - [$U(VI)_{surface}$]).

3.2 Results

The adsorption of 10 ppb U(VI) species (Figure 2a) shows typical anion-like behavior with higher adsorption at lower pH; this is consistent with the dominant aqueous species [$UO_2(CO_3)_3^{4-}$ and $UO_2(CO_3)_2^{2-}$] identified previously for dissolved U(VI) at these pH and oxidizing conditions and with the experimental results of Waite et al. (1994). In that study, adsorption of U(VI) to ferrihydrite, a microcrystalline hydrous iron oxide, was measured over a wide pH range, and surface complexation modeling was used to determine the composition and charge of the adsorbing U(VI) species. In contrast to the anionic adsorption observed in this study at pH 8.3, the dominant aqueous species of dissolved U(VI) are positively charged (Langmuir 1978) charged at low pH,

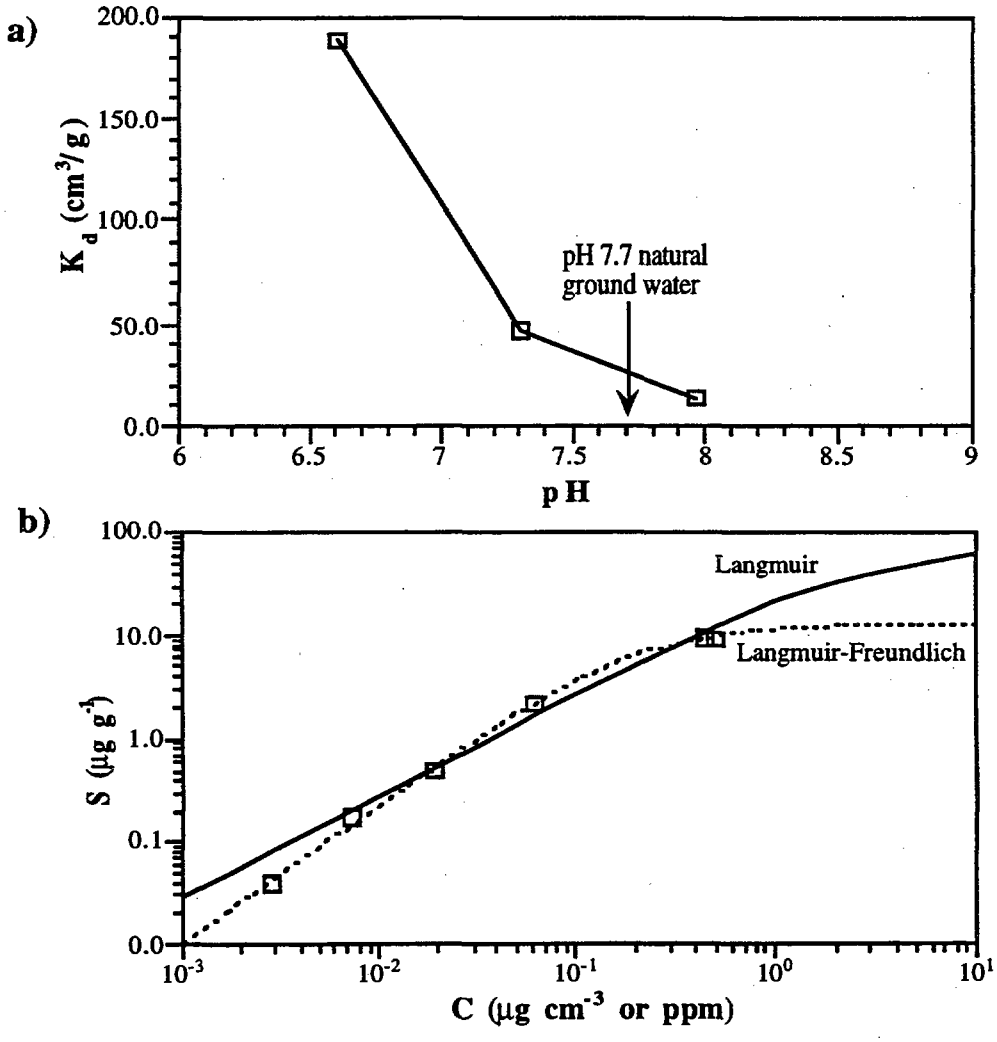

Figure 2. Uranium Mobility Under Natural (oxic) Conditions with 100 H Area Sediment Shown by: a) adsorption of U(VI) species at different pH, b) adsorption at different U(VI) species concentration

and cationic adsorption increases with increasing pH. This adsorption behavior has been observed on ferrihydrite (Waite et al. 1994) and smectite clay (Turner et al. 1996). Thus, uranium adsorption behavior over a wide pH range incorporates cationic species behavior at low pH (adsorption increasing above pH 4 to nearly 100% at pH 7) and anionic behavior at high pH (adsorption decreasing to 0% above pH 9). Geochemical surface complexation modeling was used to identify the U(VI) species that are adsorbing to the single mineral surfaces present in those studies.

Because the natural sediment used in this study contains several reactive iron phases, the U(VI)-carbonate species are likely adsorbed to several mineral surfaces present in the 100 H sediment. Previous mineralogical experiments (Amonette et al. 1994; Fruchter et al. 1996) have identified specific iron-oxide phases (amorphous and crystalline iron oxides) and clays that are involved in the iron reduction and oxidation reactions discussed. These highly reactive phases are present in low concentrations in a matrix of mainly nonreactive quartz, feldspar, and basalt minerals. It was beyond the scope of this study to determine which mineral phases were primarily responsible for the uranium adsorption in oxic systems. Solution and surface speciation analysis for these oxic samples indicated that all solution and surface species were U(VI), so adsorption (not reduction/precipitation) was assumed responsible for removal of U(VI) species from solution.

The uranium adsorption to the a single 100 H sediment in this study was significantly greater than average adsorption observed in other studies in a range of Hanford sediments. For the sediment used in this study (well H5-8 at 44 to 45 ft,<4.7 mm), a $K_d = 28$ cm^3/g was estimated (Figure 2a) at the groundwater pH of 7.7. In contrast, average uranium adsorption in shallow Hanford sediments was 0.6 cm^3/g in natural oxic water at low ionic strength (whole sediment) (Kaplan and Serne 1995). This average is based upon an earlier batch study in which U(VI) adsorption was 2.4 ± 0.6 cm^3/g (< 2 mm) (Serne et al. 1993) and an earlier column study in which U(VI) adsorption was 0.08 to 2.81 cm^3/g.[a] Although the average U(VI) adsorption was significantly lower than observed, one shallow sediment had greater adsorption ($K_d = 79 \pm 26$ cm^3/g) (Serne et al. 1993) than observed in this study, which may have been caused by high clay content in this sediment. These results illustrate the importance of characterization of the spatial variability of adsorption to accurately predict the far-field migration of a U(VI) plume.

A second batch experiment was conducted at other U(VI) concentrations (10–1000 ppb) (Figure 2b) to determine whether adsorption differs at high concentration. A linear adsorption isotherm (2) can fit the low concentration data but fails to approach the observations at 1 ppm, indicating the importance of site limitations. These data were fit with a Langmuir adsorption isotherm (5) that assumes adsorption of a single species to a single type of adsorption site. The adsorption affinity was relatively well defined (0.35 cm^3 μg^{-1}), but the adsorption maximum was poorly defined (80 μg g^{-1}). A second fit using a Langmuir-Freundlich adsorption isotherm (7) provided a better fit to the data with a slightly nonlinear slope at low concentration (slope = 0.74), which indicates heterogeneous adsorption with differing average adsorption affinity at differing concentrations. The Langmuir-Freundlich isotherm had a well defined average affinity of 5.0 cm^3 μg^{-1} and poorly defined adsorption maxima of 13 μg g^{-1} . This isotherm data indicate that if a large mass of U(VI) were released from the reduced sediment as it was oxidized, the uranium would be attenuated considerably and high concentration peak(s) would be reduced.

(a) Lindenmeier CW, RJ Serne, JC Conca, and AT Owen. 1994. Column Studies of U(VI) Transport in Hanford Sediments. Unpublished data collected at Pacific Northwest National Laboratory, Richland, Washington.

4.0 Uranium Immobilization in Reducing Aquifer Conditions

As dissolved U(VI) species in oxic or partially oxic groundwater encounters the permeable redox barrier containing reactive adsorbed Fe(II) and surface Fe(II) species, dissolved oxygen is stripped out of solution, and the dissolved uranium is reduced and precipitates as U(IV) species, as previously discussed. In this section, processes that affect the quantity and rate of uranium immobilization are assessed, including the iron redox reactions and the reduction/precipitation rate of uranium in the reduced sediment.

4.1 Batch and Column Experimental Methods

A series of batch and column experiments was conducted to determine the mass and rate of reduction of iron in sediment by the reduction solution (sodium dithionite pH buffered to 11.0). Other batch experiments were then conducted using the reduced sediment to determine the removal rate of uranium species from solution in these reducing conditions. Batch sediment reduction experiments consisted of a series of septa-top vials in which 6.0 g of sediment was mixed with 10 mL of dithionite solution for a specified time (minutes to tens of hours), then the solution was filtered and analyzed for dithionite remaining in solution. The dithionite solution contained 0.06 mol L^{-1} sodium dithionite (also called sodium hydrosulfite, $Na_2S_2O_4$), 0.24 mol L^{-1} K_2CO_3, and 0.024 mol L^{-1} $KHCO_3$. These batch experiments were conducted inside an anaerobic chamber to prevent the dithionite from reacting with oxygen. The dithionite concentration was measured by UV absorption at 315 nm. Two reactions were studied, reduction of iron in the sediment, which has a half-life of ~5 hours, and a disproportionation reaction with a half-life of 27 hours. Based on the rate of these reactions, batch reduction experiments were completed within 60 hours.

Sediment reduction studies were also conducted in 1-D columns. These experiments consisted of injecting the dithionite solution at a steady rate into a sediment column and measuring the concentration of dithionite over time in the effluent (details in Szecsody et al. 1998a) for 48 to 120 hours. The flux rate was chosen to achieve specific residence times of the dithionite solution in the column (2 to 14 hours) relative to the reaction rates. The dithionite concentration in the effluent was measured once per hour using an automated fluid system and data logging equipment.

The rate of U(VI) species removal from solution was studied in batch experiments in which 2 g of sediment was initially fully reduced in batch vials as described above. The reduced sediment and dithionite solution was then centrifuged (5000 rcf, 15 minutes), supernatant removed, an oxygen-free synthetic groundwater solution (described in section 3.1) added, and sediment resuspended. This soil washing procedure was repeated three times to remove nearly all the dithionite solution. The reduced and washed sediment was then mixed with 10 mL of U(VI)-carbonate solution. These vials sacrificed and uranium remaining in solution and on surfaces was analyzed at times ranging from minutes to 100 hours. Given that the uranium analyzer used in these studies (Brina and Miller 1993, Appendix) measures U(VI) species in solution, a series of chemical treatments was used to measure U(VI) and U(IV) in solution and on the sediment surface, as described in Section 3.1.

4.2 Sediment Reduction Studies

A study of the reduction and oxidation of iron in natural sediments by dithionite (Szecsody et al. 1998a) provided mechanism information that was needed to explain uranium remobilization during oxidation. The reduction of surface iron by sodium dithionite in batch systems (Figure 3a) has shown that a third-order reaction for the reduction of iron is needed to describe the data:

$$S_2O_4^{-2} + 2 \equiv Fe^{3+} <==> 2 \equiv Fe^{2+} + SO_3^{-2} + 2H^+ \quad (14)$$

in comparison to a first-order approximation of this reaction with the assumption that $\equiv Fe^{3+}$ remains constant and can be considered constant:

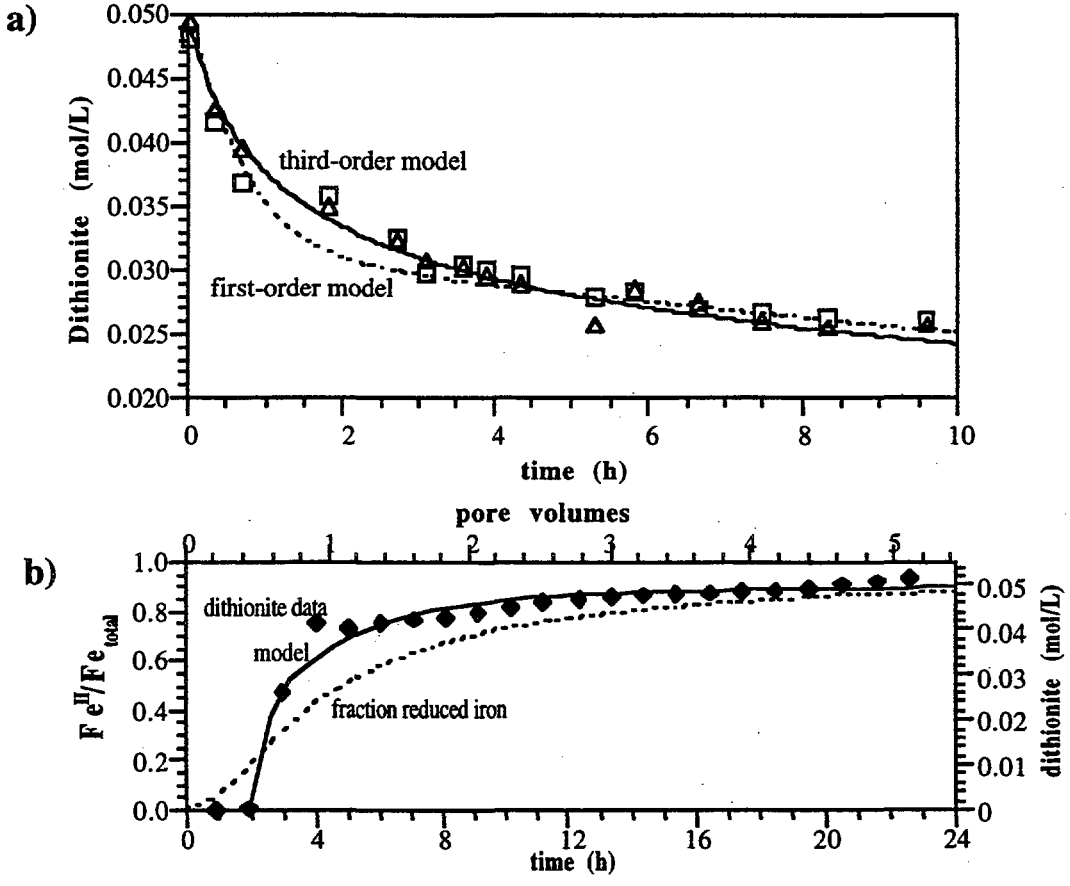

Figure 3. Processes Controlling Uranium Immobilization in Reduced Aquifer Conditions: a) rate of U(VI) reduction and precipitation in contact with dithionite reduced sediment (batch experiments and simulation), b) rate of iron reduction in sediment shown by 1-D column experiment with sodium dithionite injection and slow approach to equilibrium

$$S_2O_4^{-2} \quad <==> \quad 2 \equiv Fe^{2+} + SO_3^{-2} \tag{15}$$

Reaction (15) is reasonably valid for injections in which the iron is in far excess of the dithionite. A second reaction is also needed for this system that describes the disproportionation of dithionite in contact with sediment:

$$2S_2O_4^{-2} + H_2O \quad <==> \quad S_2O_3^{-2} + 2HSO_3^- \tag{16}$$

Reduction of Hanford sediment was matched with reactions (14) and (16), indicating the importance of the limited number of reducible iron sites in describing the reaction rate. The rate of reduction of sediment had a half-life of ~5 hours.

Reduction of iron in sediment during transport is shown by a 1-D column experiment (Figure 3b) in which the initial fast breakthrough of dithionite is followed by a slow approach to equilibrium. Reactions (14) and (16) were needed to fit these data (i.e., a simpler approach; reactions 15 and 16 could not fit the data). In addition to the two chemical reactions, a slow physical approach to equilibrium was needed. In a column experiment of the breakthrough of dissolved oxygen in a nonreduced sediment (not shown), the slow approach to equilibrium (relative to a tracer) indicated that a fraction of the sites were slower to be accessed. Based on this result, a diffusion step was added for a fraction of the iron sites

$$S_2O_4^{-2} + 2 \equiv \equiv Fe^{3+} \quad <==> \quad 2 \equiv \equiv Fe^{2+} + SO_3^{-2} + 2H^+ \tag{17}$$

where the total number of oxidized or reduced iron sites is the sum of sites in reactions 14 and 17.

4.3 Uranium Immobilization by Reduced Sediment

The removal of U(VI)-carbonate species added to reduced sediment was mainly by precipitation, so it was not dependent on the type of reduced iron species present on the sediment surfaces. Batch time-course experiments were conducted at two initial U(VI) concentrations (10 and 100 ppb) (Figure 4), both of which decreased in concentration to the solubility limit in anoxic systems. These results are in good agreement with the solubility results of others (Rai et al. 1990; Cantrell et al. 1995). The solid line (Figure 4) represents the solubility limit of amorphous $UO_2 \cdot xH_2O$ under reducing conditions in contact with metallic iron or $EuCl_2$ as a reductant (Rai et al. 1990). The dashed line represents the maximum extent of the scatter of their solubility values. In a different study of metallic iron particles as potential permeable barrier material (Cantrell et al. 1995), similar immobilization of uranium was also observed (also plotted in Figure 4), indicating that the solubility limit was controlling the aqueous uranium and that there was little influence of the specific type of reduced surface sites.

The rate of removal of U(VI)-carbonate species (Figure 4) was within minutes, and the reaction used considered the uranium removal from solution as a precipitation reaction:

$$UO_2(CO_3)_3^{4-} \quad <==> \quad UO_2 \tag{18}$$

This first-order reaction was fit to the 10 ppb uranium data with a half-life of three minutes.

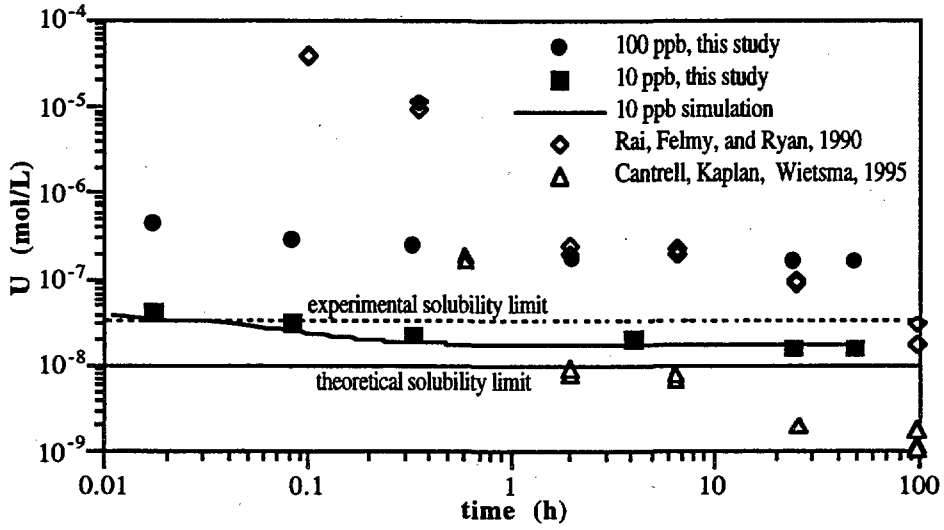

Figure 4. Rate of Removal of U(VI)-Carbonate Species at 10 and 100 ppb in Contact with Dithionite-Reduced Sediment. The Eh of the solution in contact with this sediment is -560 mV; simulation of 10 ppb data (shown) is with a 3-minute half-life. Data from other studies shown are in anoxic systems that are not as reducing as the sediments in this study.

Because some U(IV)-containing precipitates are not homogeneous and may contain both U(VI) and U(IV), sediment samples from this batch experiment were analyzed for the presence of U(VI) and U(IV) species in the uranium precipitates, as described in Section 4.1. All of the surface samples in these reduction experiments contained U(IV) species. It was assumed that UO_2 was formed by precipitation in these experiments.

5.0 Uranium Remobilization During Aquifer Oxidation

The U(IV) precipitate that forms on the reduced sediment will remobilize into solution when the reductive capacity of the permeable barrier is exhausted and the reduced iron in the aquifer sediment is oxidized by dissolved oxygen in the groundwater. The rate of uranium remobilization depends on several reactions or processes, including the oxidation rate of the reduced Fe(II) barrier, the oxidation rate of U(IV) species, and aging of the U(IV) precipitate-sediment assemblage. Experiments to quantify these processes and transport modeling to simulate the predicted uranium movement under field conditions are described in this section.

5.1 Batch and Column Experimental Methods

The rate at which the dithionite-reduced sediment was oxidized was studied in 1-D columns. These experiments consisted of injecting oxygen-saturated (8.2 mg L^{-1} or 256 μmol L^{-1}) synthetic groundwater (Section 3.1) at a steady rate into a reduced sediment column and measuring the concentration of dissolved oxygen over time in the effluent (details in Szecsody et al. 1998a) for 100 to 3200 hours. The flux rate was chosen to achieve specific residence times of the dissolved oxygen in the column relative to the oxidation rate(s) of the sediment.

The rate of U(IV)-species release into solution was studied in batch experiments in which 2 g of uranium precipitate on reduced sediment was initially prepared as described in Section 4.1 and the oxidation experiments conducted immediately. These batch oxidation studies were conducted for the following initial conditions: a) 10 ppb U(VI) initially in solution at pH 8.6, b) 10 ppb U(VI) initially in solution at pH 8.2, and c) 100 ppb U(VI) initially in solution at pH 8.2. Each experiment consisted of six to eight separate sealed vials in which oxidation is initiated by opening each tube in an oxygen-rich environment. There was enough excess oxygen in the headspace of each vial to fully oxidize the sediment. Vials were not kept open to prevent losses from evaporation, which would have complicated the results. Vials were then rotary-mixed and sacrificed at specific times ranging from 1 to 800 hours and analyzed for solution U(VI) and U(IV) species, as described in Section 4.1.

Long contact times of uranium precipitates with sediment can lead to slower uranium release rates when the sediment is oxidized (Payne et al. 1994). The aging effect was examined by conducting additional batch experiments in which there were 170 and 1000-hour contact times of the uranium precipitate and reduced sediment before the oxidation experiments were conducted. With these relatively short time scales, there is likely little iron oxide recrystallization compared with what occurs in field systems with decades of contact time, but these experiments provided an indication of the importance of this aging process.

5.2 Sediment Oxidation Studies

The release of reduced uranium into solution will begin when the reduced sediment-water system is oxidized such that the Eh is greater than 0.0 V (Garrels and Christ 1965). Although the uranium release is caused by the dissolution of the uraninite, the rate of this release is controlled partially by the oxidation rate of the reduced iron, because it mainly controls the redox conditions.

In most field systems of interest, the main oxidant for reduced iron is dissolved oxygen in water, and the rate of iron oxidation at pH 8 (see Section 2.3) has been reported as seconds for pure iron oxides (Buerge and Hug 1997). However, for the natural sediments of this study, which contain multiple iron oxide phases, the sediment oxidation rate is considerably slower and the mechanism likely more complex than a single reaction.

A study of the reduction and oxidation mechanisms of the sediments (Szecsody et al. 1998a) showed that a large fraction of the sediment is oxidized within an hour, but hundreds of hours are needed to fully oxidize the sediment. This concept is illustrated by three oxidation column experiments at differing pore water velocities (Figure 5a–c) in which the slowest velocity (Figure 5a) shows dissolved oxygen remaining low for 370 pore volumes, after which oxygen saturation is quickly achieved. This equilibrium breakthrough curve shape is caused by the oxidation reaction rate being considerably faster than the residence time in the column (60 hours), therefore, dissolved oxygen had time to fully react with reduced iron. At a velocity at which dissolved oxygen only partially reacts with reduced iron (Figure 5b, residence time 1.9 hours), dissolved oxygen breakthrough rises after 100 pore volumes, then slowly approaches oxygen saturation. At a higher velocity (Figure 5c, residence time 0.2 hours), partial oxygen breakthrough occurs almost immediately, followed by the slow approach to oxygen saturation over hundreds of pore volumes. A rough approximation of the sediment oxidation rate half-life is 0.25 hour, based on the dissolved oxygen plateau in Figure 5c (10–60 pore volumes).

The oxidation of reduced iron in the natural sediment appears to be more complex than a single oxidation reaction and is likely controlled by both chemical and physical processes. A reactive transport model was used to simulate the oxidation of the sediment with a single reaction:

$$4{\equiv}Fe^{2+} + O_2 + 4H^+ \text{ <=> } 4{\equiv}Fe^{3+} + H_2O \qquad (19)$$

which is the stoichiometric addition of reactions 5 through 7. This single reaction could not fit the dissolved oxygen breakthrough data shown in Figure 5c, which contains multiple slope changes. However, with the addition of a second type of reduced iron

$$4{\equiv\equiv}Fe^{2+} + O_2 + 4H^+ \text{ <=> } 4{\equiv\equiv}Fe^{3+} + H_2O \qquad (20)$$

that dynamic breakthrough curve shape can generally be fit using both reactions 19 and 20 (line shown in Figure 5c). This simulation had 20% of the reduced iron is modeled with reaction 20 with a considerably slower rate. The breakthrough curve shape is not well fit initially (0 to 20 pore volumes), and a more complex approach for reaction 19 is needed. Breakthrough curve tailing in a column experiment of purely dissolved oxygen in a nonreduced sediment (not shown) for 5 - 6 pore volumes indicates diffusional limitations accessing a fraction of the pore volume. This physical tailing for dissolved oxygen could explain the tailing observed for dissolved oxygen for the fast oxidation reaction (Figure 5c, 10 - 40 pore volumes). Measurement of the column effluent Eh (Figure 5d, same experiment as Figure 5b) also provides an indication of the complexity of the oxidation of the sediment.

Iron extractions conducted on unreduced and reduced sediments indicate that there is more than one type of reduced iron present on the surface (Szecsody et al. 1998a). The total iron (II+III) oxides and carbonates of a sediment sample tested was 0.14% of the sediment by weight. Of these iron phases, ~85% were Fe(III) oxides, 2.4% was $Fe(II)CO_3$, and 9% other Fe(II) species.

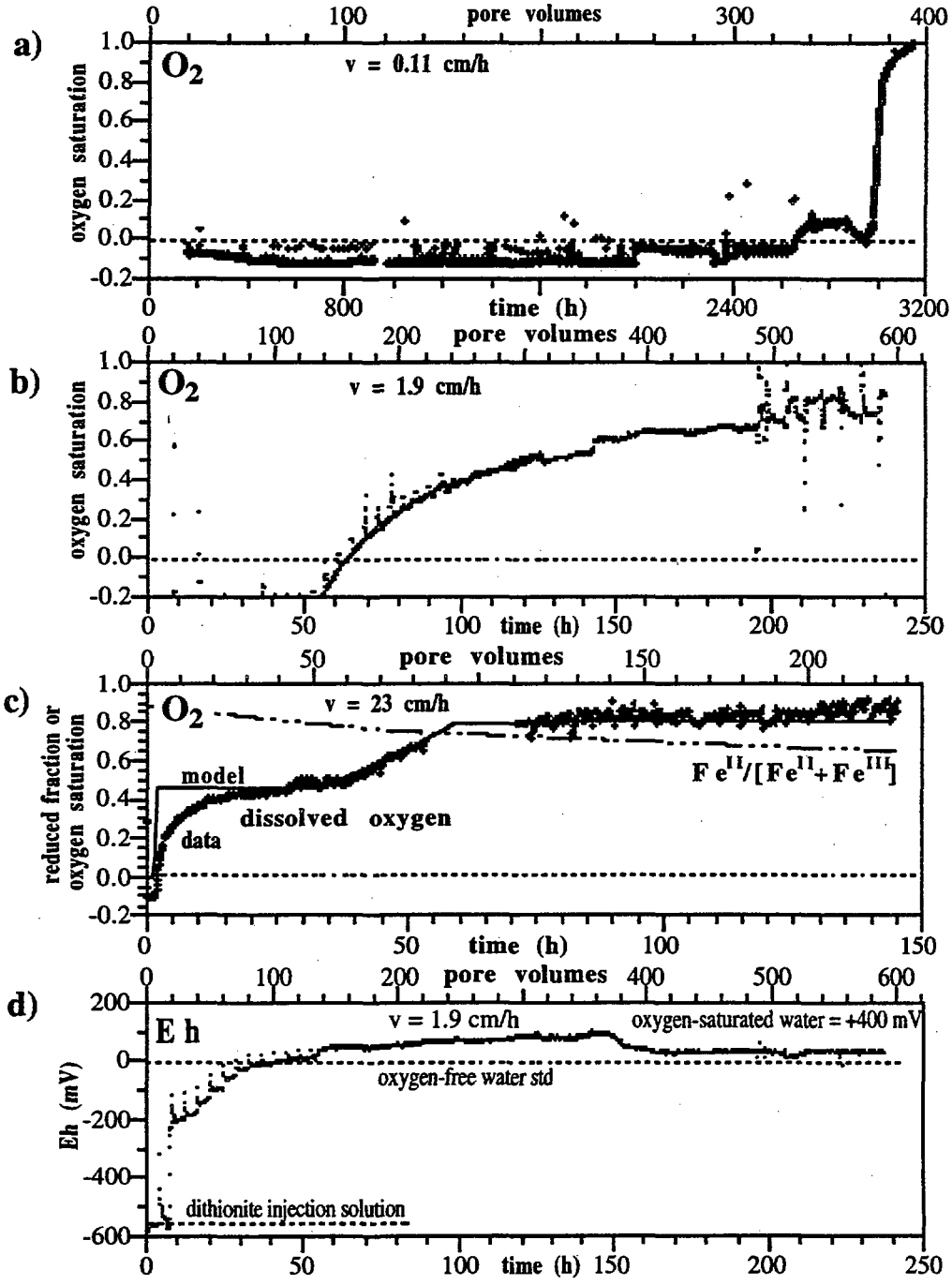

Figure 5. Oxidation of Dithionite-Reduced Sediment by Dissolved Oxygen in Water (8.2 mg/L) in Three 1-D Column Experiments with Differing Velocities Resulting in Different Contact Times of Dissolved Oxygen with Adsorbed Fe(II) in the Sediment: a) 60-, b) 1.9-, and c) 0.2-hr residence times. Oxidation simulated with a model that considers fast and slow oxidation by dissolved oxygen (reactions 19 and 20) as shown in (c) for dissolved oxygen and fraction of reduced iron. The Eh of the effluent solution during sediment oxidation (d, same experiment as b) also illustrates partial oxidation of a fraction of the surface sites.

Dithionite treatment resulted in the sediment containing 80% ion exchangeable F(II) (i.e., adsorbed to the surface) and 9% $Fe(II)CO_3$. Subsequent oxidation of the sediment by dissolved oxygen resulted in oxidation of all the ion-exchangeable Fe(II) and half of the $Fe(II)CO_3$. Thus quickly oxidizing sites may represent adsorbed Fe(II) and slowly oxidizing sites may represent $Fe(II)CO_3$, which is considerably slower to oxidize by dissolved oxygen. In addition, a small percentage of the reduction capacity (< 4%) of the sediment is due to Mn(II).

5.3 Uranium Mobilization Experiments

U(IV) oxidation (i.e., remobilization) experiments were conducted under a range of geochemical conditions likely to be encountered in the field. Batch experiments were conducted with a 24-hour contact time of the U(IV) precipitate and reduced sediment, pH 8.2 to 8.5, and 10 to 100 ppb initial U(VI) concentration (Figure 6a). The experiments at 10 ppb initial U(VI) species concentration and pH 8.2 and 8.6 showed that the oxidation rate had a 100–300-hour half-life. Uranium mining literature supports the conclusion that U(IV) oxidation rates are slow in high-pH carbonate systems (Pearson and Wadsworth 1958). The experiment with 100 ppb U(VI) initially showed a slower oxidation rate.

The oxidation of uraninite by dissolution was modeled as requiring dissolved oxygen in order to create the condition that the Eh needed to be greater than 0.0 V for uraninite oxidation to occur:

$$UO_2 + O_2 \iff UO_2(CO_3)_3^{4-} \qquad (21)$$

This reaction proceeded very slowly at first, and most of the dissolved oxygen was used up by the reduced iron (reactions 19 and 20). After most iron sites were oxidized and some dissolved oxygen was in solution, uranium oxidation proceeded. Thus the general shape of the uranium release was small from 0.5 to 10 hours with the major release at 50 to 300 hours. The uranium simulation provided a relatively good fit to the pH 8.2 data (line shown, Figure 6a) with a half-life of 200 hours for this second-order reaction. At 100 ppb initial U(VI) concentration, the rate was slower (450-hour half-life). Given that the U(IV) precipitates will be in contact with sediment for decades, slower oxidation rates are expected because precipitates are slowly incorporated into metal-oxide structures. This formation of stronger uranium surface bonds over time has been reported for U(IV) species (Payne et al. 1994) and was the subject of a second series of oxidation experiments in which the U(IV) reduced sediment contact time was varied from 24 hours to 170 hours to 1000 hours before oxidation (Figure 6b). Although there was no difference between the 24 and 170-hour experiments, the 1000-hour data indicated a slower oxidation rate.

The combined rate of Fe(II) and U(IV) species oxidation result in an observed U(IV) release rate to solution that is slower than the U(IV) oxidation rate alone. A simulation was conducted of the two-reaction Fe(II) oxidation rate (80% [reaction 16] with a half-life of six hours, 20% [reaction 17] with a 120-hour half-life) coupled with the U(IV) oxidation rate (200-hour half-life) (Figure 6c) . These results show that uranium release to solution slows at later times as the release rate becomes limited by the slowly oxidizing Fe(II) sites. Given these slow release rates, uranium concentrations are not expected to reach high levels upon barrier oxidation.

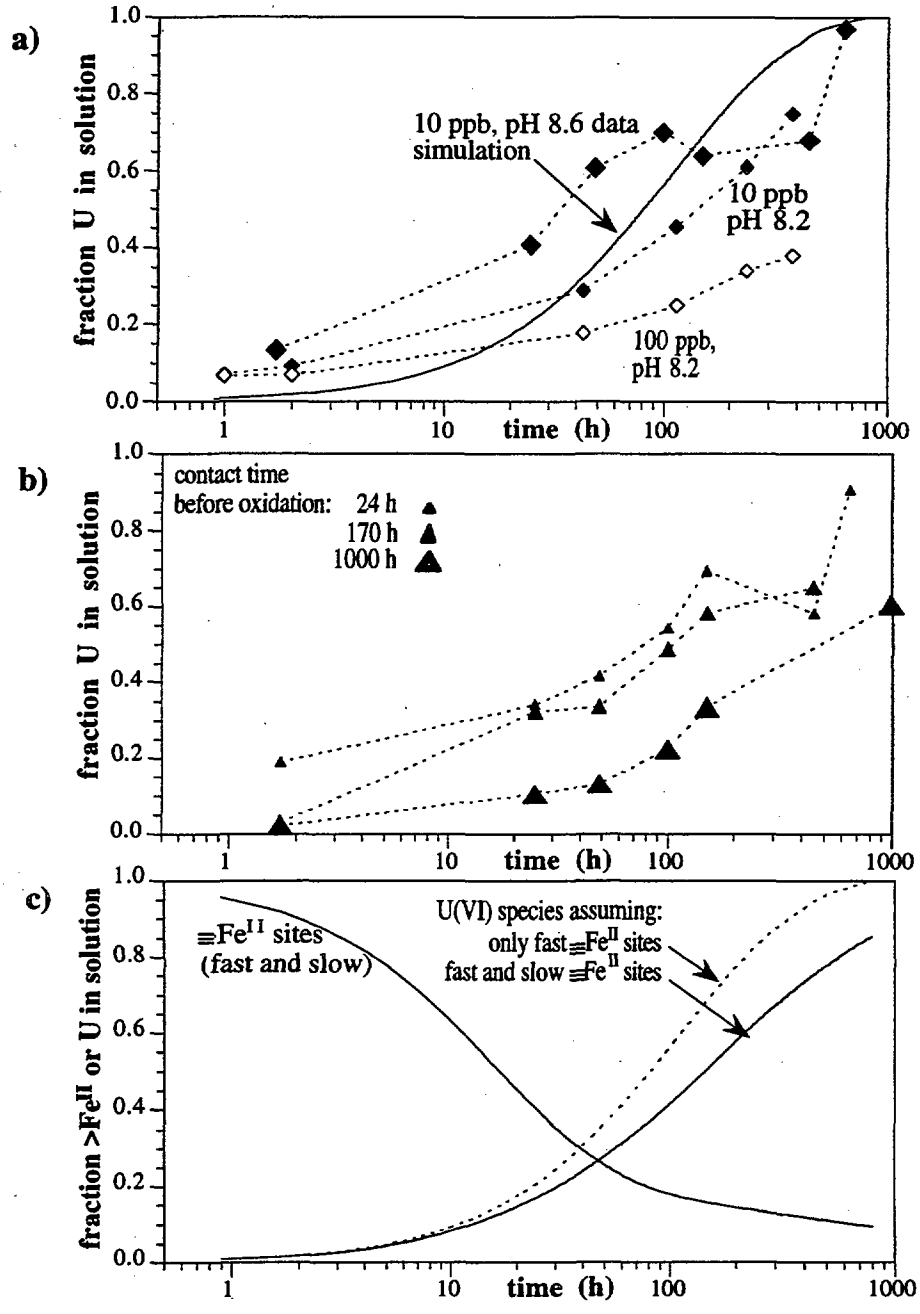

Figure 6. Uranium Release into Solution as Hanford Sediment Is Oxidized. Uranium release shown for differing initial U(VI) concentrations and pH (a) and different uraninite-reduced sediment contact time before oxidation (b). The uranium data were modeled assuming two different types of iron sites (slow and fast oxidizing), which influenced the uranium release rate (c).

5.4 Uranium Transport Simulations

1-D and 2-D transport simulations were conducted to predict uranium concentrations under field conditions using reaction rates defined in laboratory experiments. Both realistic and worst-case geochemical and physical parameters were considered for these simulations. The simulations follow three conceptual steps (Figure 1): 1) dithionite is injected for a short period of time to reduce all of the available iron; 2) oxygen-saturated water containing 10 ppb U(VI) species flows through the barrier resulting in considerable accumulation of uranium; and 3) oxidation of the barrier and uranium release to solution. The reactions considered included: 1) iron reduction with one site (reaction 14), 2) dithionite disproportionation (reaction 16), 3) uranium reduction/precipitation (reaction 18), 4) sediment oxidation with one site (reaction 19), and 5) uranium oxidation (reaction 21), and 6) retarded transport of U(VI) species (Langmuir 1978, reaction 5). The oxidation rate of the Fe(II) barrier was assumed to be fast (i.e., using the six-hour oxidation rate only, no slow oxidizing sites) to represent a worst case. The reactive transport model (described in Section 2.4) incorporated these reactions with the parameters described in the preceding sections. The U(VI) species oxidation rate was varied in simulations from 200 hours or eight days (based on laboratory data) (Figure 5) to slower values (based upon published uranium mining data).

These simulations assumed horizontal flow through a 10-m-wide redox barrier (i.e., size of the reduced sediment from the 100 H Area single-well injection) and a 3-m vertical thickness for the 2-D simulations. The concentrations shown in the plots represent a location at the downgradient edge of the redox barrier, so they represent the highest concentrations that could be encountered. The flow rate used (0.1 m/day) was within the range expected for natural gradient flow in the Hanford unconfined aquifer, or 1 to 2 orders of magnitude slower than laboratory experiments. Longitudinal dispersivity was assumed to be 0.18 m, which was based on tracer transport modeling of the 100 H Area field experiment (0.25 m or 0.07 m for different formations). Simulations were conducted assuming that 10 ppb of uranium accumulated for 70 pore volumes (20 years), given that the average amount of water needed for sediment oxidation in the 100 H Area was 68±42 pore volumes (of oxygen-saturated water) based on 12 cores taken from a field-scale reduction experiment.

Simulation of uranium transport using these conditions indicated that the U(VI) species concentration would peak at 35 ppb within two years after the barrier was oxidized (Figure 7a, solid line, which represents a simulation using parameters considered most accurate). The eight-day (200-hour) oxidation rate is highly likely to represent the fastest rate that would be observed in the field (based on immediate oxidation after precipitation); field oxidation rates are likely to be slower due to sediment aging. Several additional simulations were conducted to determine the sensitivity of the uranium peak concentration to key parameters. A decrease in the U(IV) oxidation rate from eight to 800 days decreased the uranium peak concentration to 20 ppb. The uranium peak concentration was relatively insensitive to this two order-of-magnitude decrease in uranium oxidation rate because the uranium release rate was largely controlled by dispersion during iron oxidation. The sensitivity of dispersion is shown by comparing simulations with different values of longitudinal dispersivity (Figure 6b) in which an artificially low value of dispersion (0.01 m) increased the peak uranium concentration to 50 ppb. Field-scale transport of the uranium plume would also be subject to 3-D spreading, which would lower uranium concentrations from the values shown in these 1-D simulations.

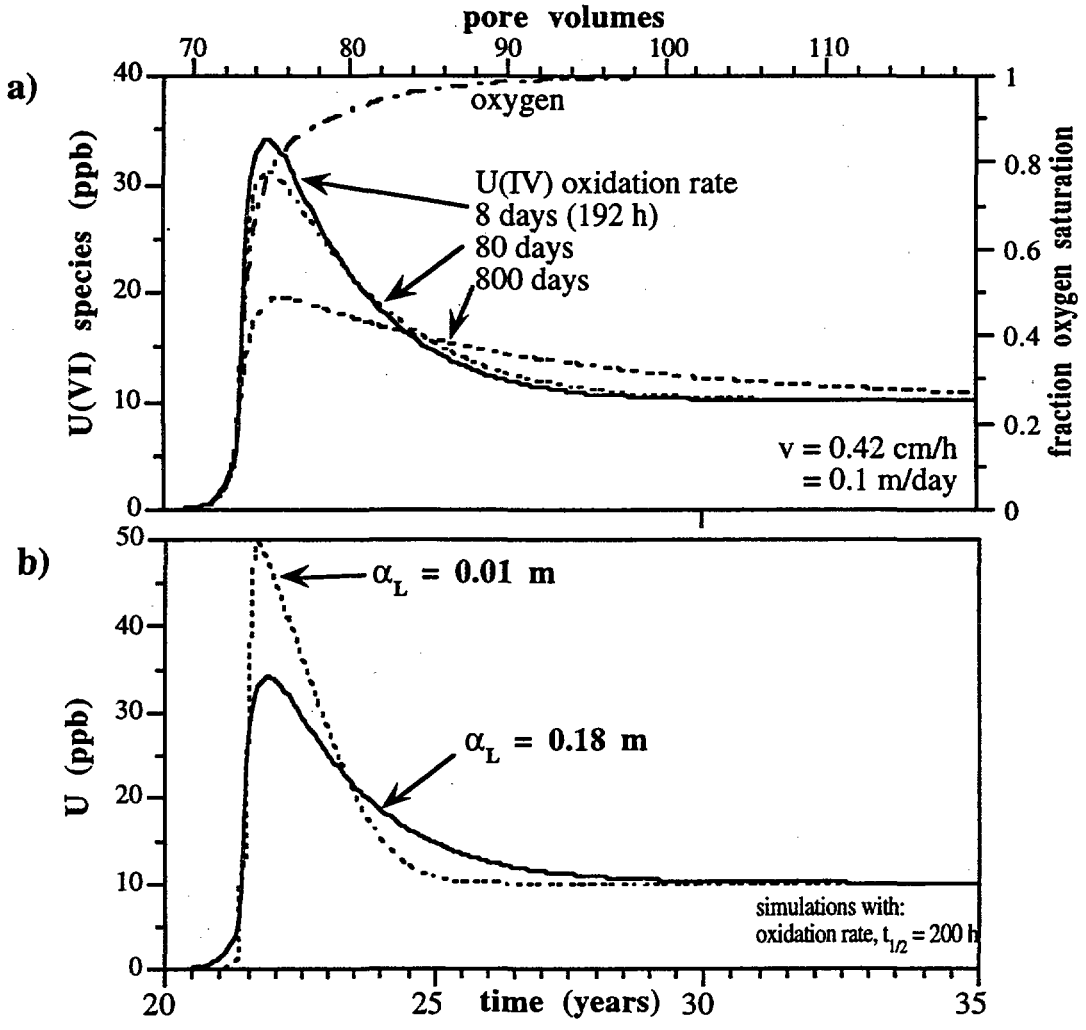

Figure 7. Simulated Uranium Mobility under Field Conditions as the Redox Barrier Is Oxidized with a) different U(IV) oxidation rates, and b) different values for longitudinal dispersivity. Assumptions for these 1-D simulations included horizontal flow at 0.1 m/day across a 10-m wide reduced iron barrier that is oxidized in 20 years (70 pore volumes).

6.0 Uranium Remobilization in the Presence of Chromate

6.1 Experimental Methods

Placing the redox barrier in the 100 D area of the Hanford Site is expected to prevent chromate present in the shallow aquifer from reaching the Columbia River. Chromium is a redox-sensitive contaminant that will be immobilized, like uranium, at the redox barrier as a result of precipitation reactions when Cr(VI) is reduced to the less soluble Cr(III) (reaction 13). Although the reduction of chromate oxidizes Fe(II), because most chromate contamination is <5 ppm, dissolved oxygen is mainly responsible for oxidizing the Fe(II). Chromate would need to be present at a concentration of 41 mg/L to be as able to oxidize the redox barrier as dissolved oxygen is. Therefore, while chromate oxidation of the reduced sediment and the subsequent effect on uranium transport was not considered likely, because chromate is a stronger oxidant than dissolved oxygen, it may have some impact on the barrier oxidation rate even if present at a low concentration. Chromate transport behavior was also studied because of the relative difference in mobility compared with uranium species. Cr(III) is not readily oxidized to Cr(VI) when the redox barrier is ultimately oxidized. To test this difference in behavior, a long-term column experiment was conducted in which both U(VI) and Cr(VI) were injected through reduced sediment and the remobilization behavior monitored once the sediment was oxidized.

The column experiment was conducted by injecting near oxygen-saturated water (average of 6.0 mg L^{-1}), 2.3 mg L^{-1} Cr (as chromate), and 10 μg L^{-1} U(VI) into a reduced sediment column until the sediment column was oxidized. This 4000-hour (six-month) experiment was conducted with Hanford formation sediment that was treated with the reductant in a method similar to that used at the field scale (sodium dithionite injected for 12 hours, then a 48-hour no-flow interval). Over the 4000-hour interval of the experiment, the U(VI) injection concentration was stepped (7 ppb, 0–1500 hours; 30 ppb, 1500–4000 hours) and CrO_4^{2-} injection concentration was near the maximum used in the 100 D area (2.30 ppm).

6.2 Results

Results of the column experiment showed that the presence of 2.3 ppm chromate did not increase the rate of U(VI) release to solution. The breakthrough of dissolved U(VI) in this experiment (Figure 8a) occurred without a concentration peak, as shown in Figure 8, indicating that the combination of redox reactions slowly released U(VI) aqueous species to solution. The U(VI) aqueous species will adsorb (Figure 1) once remobilized, but this will amount to only a 40-pore volume lag based on the conditions of this column experiment. Thus the uranium data indicate that oxygen breakthrough occurred at 1400 to 1600 hours (600 pore volumes). After 1500 hours, the U(VI) effluent values matched influent values, suggesting that there was no significant redox capacity remaining in the sediment. Comparing the mass of dissolved U(VI) injected (0.326 mg) with the mass recovered in the effluent (0.303 mg) indicates 93% mass recovery.

This experiment also confirmed the expected difference in behavior of U(IV) and Cr(III) species. Chromate transport was similar to that of U(VI), with breakthrough near 1500–2000 hours when the sediment was no longer redox-reactive. However, the mass of injected chromate (CrO_4^{2-}) (42.7 mg) was not recovered even after 4000 hours (effluent was 20.7 mg or 48%) (Figure 8b). This was expected due to the slow dissolution rate for solid $Cr(OH)_3$ in oxic water.

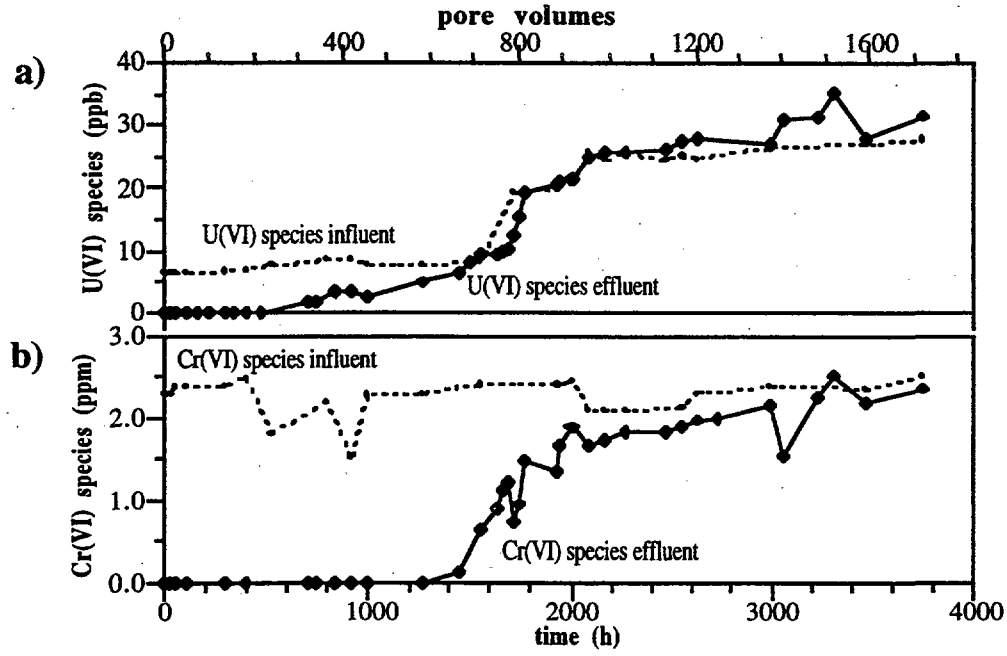

Figure 8. Column Experiment Results of Remobilization of U(VI) Species (a) and Cr(VI) Species (b) During Transport in, as Sediment Is Oxidized by Dissolved Oxygen

7.0 Conclusions

The purpose of this study was to assess uranium mobility issues during the life cycle of an in situ redox manipulation process that is being implemented for remediation of chromate-contaminated sediment at the 100 Areas of the Hanford Site (Fruchter et al. 1996). Processes that controlled the mobility of uranium during reduction and oxidation of the Hanford sediment were studied in static (batch) and dynamic (1-D column) laboratory experiments and coupled chemical/physical processes simulated with a multireaction transport model. These studies were conducted to determine uranium mobility in 1) natural oxic groundwater systems, 2) a reducing environment created by the chemical reductant (sodium dithionite), and 3) an oxic environment created when the reduced sediment is oxidized by dissolved oxygen.

Experiments defining uranium transport in the natural oxic sediment indicated that if a large release of uranium occurred from a reduced zone, its movement would be retarded and spread out due to adsorption. An adsorption isotherm showed that the adsorption maximum was about three orders of magnitude greater than the naturally occurring U(VI) concentration (10 ppb). The adsorption of U(VI) species was nonlinear over a wide concentration range, indicating more than one type of adsorption site and/or adsorbing species. This result is consistent with the fact that 1) multiple U(VI) species are present [60% $UO_2(CO_3)_3^{4-}$, 30% $UO_2(CO_3)_2^{2-}$, 10% $(UO_2)_3(OH)_5^{+}$] that showed anionic adsorption behavior, and 2) the sediment contains multiple iron oxide phases that serve as adsorption sites. The importance of characterization of the spatial variability of adsorption to predict far-field U(VI) migration is shown by other studies that report U(VI) adsorption values three times more to 10 times less than values in this study (the average is significantly less) (Serne et al. 1993).(a)

When oxic groundwater containing U(VI) species flows through a reduced sediment zone, uranium species are reduced and precipitate as U(IV) species (presumed to be uraninite, UO_2) within minutes. The reduction rate (half-life three minutes) was experimentally determined in batch systems with 10 and 100 ppb U(VI) species initially in solution. The final concentration was near the solubility limit for uranium in reducing environments at pH 8. Although literature indicates some mixed U(IV, VI) precipitates can occur, our analysis indicated only U(IV) species. This may be caused partially by the highly reducing environment considered in this study (Eh ~-0.5 V), which was also investigated experimentally. When the sediment is treated chemically with dithionite buffered at high pH, amorphous and some crystalline iron oxides are dissolved/reduced, forming mainly adsorbed Fe(II) and some $Fe(II)CO_3$. In addition, a small fraction (<4%) of the reduction capacity of the sediment is due to Mn(II).

The amount of uranium accumulation in the reduced sediment zone depends on the mass of reduced iron as well as the mechanisms that eventually oxidize the zone. The mass of dithionite-reduced iron ranges from 0.05 to 0.4% for the Hanford sediments tested. Oxidation of this sediment occurs by 1) advection of dissolved oxygen in groundwater; 2) advection of other oxidants, such as chromate, in groundwater; and 3) diffusion of oxygen in the vadose zone for sediments near the water table. Dissolved oxygen in water is considered the main oxidant in this study

(a) Lindenmeier CW, RJ Serne, JC Conca, and AT Owen. 1994. Column Studies of U(VI) Transport in Hanford Sediments. Unpublished data collected at Pacific Northwest National Laboratory, Richland, Washington.

because chromate would need to be present in very large (>120 ppm) concentrations to be as effective. The vertical extent of oxidation by diffusion is only a few feet even after decades. Uranium accumulation would vary with the spatial variability of the reduced iron content. A field-scale estimate of the 10-ppb U(VI) accumulation is ~70 pore volumes over 20 years based on cores taken from a 100 H field reduction test in 1995 that showed 68±42 pore volumes of oxygen-saturated water were needed for oxidation. Based on relatively high estimates of groundwater flow rates in the 100 D and H areas, it was estimated that this reduced zone would last approximately 20 years. There is a wide variability in the amount of iron in sediments, as shown by a long-term column experiment in which 800 pore volumes of oxygen-saturated water were needed for sediment oxidation. Uranium release simulations in this study were based on the amount of uranium accumulation in 68 pore volumes of water over a 20-year period.

Although U(IV) precipitates on surfaces, geochemical processes release uranium slowly to solution once the redox barrier is oxidized. The release of uranium back into solution is controlled by 1) the U(IV) oxidation rate, 2) the sediment oxidation rate, and c) the dispersion of the uranium plume in the aquifer. The fastest rate of U(IV) oxidation observed in experiments had a 200-hour half-life, and coupled reactions likely to occur would decrease the uranium release rate. Long-time contact of U(IV) precipitates with sediment (i.e., aging) was also shown experimentally to result in slower U(IV) oxidation rates to a 450-hour half-life after a 1000–hour uraninite-sediment contact time. A likely aging mechanism is slow incorporation of precipitates into metal-oxide structures (Payne et al. 1994). The mechanism of oxidation of the reduced iron in the sediment is more complex than can be described with a single sediment oxidation reaction. The dissolved oxygen breakthrough curve shape can be modeled with a minimum of two reactions, in which one type of surface iron (80%) is oxidized quickly (~ 5-hour half-life) and a second type is oxidized slowly (~120-hour half-life). The necessity of two different surface Fe(II) sites to model sediment oxidation is consistent with measurement of two main reduced Fe(II) species by iron extraction techniques. Sediment extractions showed the natural sediment containing ~85% Fe(III) phases was altered to 80% ion exchangeable F(II) (i.e., adsorbed to the surface) and 9% $Fe(II)CO_3$ by the dithionite treatment process. Subsequent oxidation of the sediment by dissolved oxygen resulted in oxidation of all of the ion exchangeable Fe(II) and half of the $Fe(II)CO_3$. Other experimental evidence indicates that diffusional processes also have a minor effect on dissolved oxygen breakthrough curve shape, so sediment oxidation is likely controlled by multiple chemical and physical mechanisms.

Transport simulations were conducted to predict uranium concentrations under field conditions using the chemical reaction rates defined in laboratory experiments. Assumptions included horizontal flow through a 10-m-wide redox barrier, a 3-m vertical thickness, and a natural gradient flow rate (0.1 m/day). A simulation of uranium transport using the most realistic parameters indicated that the U(VI) species concentration would peak at 35 ppb within two years after the barrier was oxidized. Although field oxidation rates are likely to be slower due to sediment aging, simulations decreasing the U(IV) oxidation rate by two orders of magnitude only had a minor effect on the peak uranium concentration (20 ppb) because of the influence of the slow iron oxidation. Field-scale transport of the uranium plume would also be subject to longitudinal and lateral plume dispersion, which would lower uranium concentrations, as shown by simulations in which the longitudinal dispersivity was altered. Finally, a six-month-long column experiment with large uranium accumulations confirmed that uranium was slowly released into solution with U(VI) concentrations elevated only slightly above injected concentration. This experiment also demonstrated that another oxidant likely to be present in some field systems, chromate, did not result in a fast release rate of uranium into solution.

8.0 References

Adler HH. 1974. "Concepts of Uranium-Ore Formation in Reducing Environments in Sandstones and Other Sediments." *Formation of Uranium Ore Deposits*. Proceedings Series IAEA-SM-183/43, International Atomic Energy Agency, Vienna.

Amonette JE, JE Szecsody, HT Schaef, JC Templeton, YA Gorby, and JS Fruchter. 1994. "Abiotic Reduction of Aquifer Materials by Dithionite: A Promising In Situ Remediation Technology." *In Situ Remediation: Scientific Basis for Current and Future Technologies. Thirty-Third Hanford Symposium on Health and the Environment.* November 7-11, 1994, Pasco, Washington, GW Gee and NR Wing, eds. Battelle Press, Columbus, Ohio.

Arbogast T, A Chilakapati, and MF Wheeler. 1992. *Numerical Methods in Water Resources*, TF Russell, RE Ewing, CA Brebbia, WG Gray, and GF Pinder, eds. Computational Mechanics Publications, Southampton, UK, pp. 77-84.

Brina R and AG Miller. 1992. "Direct Detection of Trace Levels of Uranium by Laser-Induced Kinetic Phosphorimetry." *Analytical Chemistry*, 64 (13):1413-1418.

Brina R and AG Miller. 1993. "Determination of Uranium and Lanthanides in Real-World Samples by Kinetic Phosphorescence Analysis." *Spectroscopy*, 8:1-14.

Bruno J, I Casas, and I Puigdomenech. 1988. "The Kinetics of Dissolution of UO_2(s) Under Reducing Conditions." *Radiochimica Acta,* 11:44-45.

Bruno J, I Casas, and I Puigdomenech. 1991. "The Kinetics of Dissolution of UO_2 Under Reducing Conditions and the Influence of an Oxidized Surface Layer (UO_{2+x}): Application of a Continuous Flow-Through Reactor." *Geochimica et Cosmochimica Acta,* 55:647-658.

Buerge IJ and SJ Hug. 1997. "Kinetics and pH Dependence of Chromium(VI) Reduction by Iron(II)." *Environ. Sci. Technol.*, 31(5):1426-1432.

Cantrell KJ, DI Kaplan, and TW Wietsma. 1995. "Zero-Valent Iron for the In Situ Remediation of Selected Metals in Groundwater." *Journal of Hazardous Materials*, 42:201-212.

Chilakapati A. 1995. *RAFT: A simulator for reactive flow and transport of groundwater contaminants.* PNL-10636, Pacific Northwest Laboratory, Richland, Washington.

Chilakapati A, T Ginn, and J Szecsody. 1998. "An analysis of complex reaction networks in groundwater modeling."*Water Resour. Res.*, 34(7):1767-1780.

Frondel C. 1958. *Systematic Mineralogy of Uranium and Thorium*. Bulletin 1064, U.S. Geological Survey, Washington, D.C.

Fruchter JS, JE Amonette, CR Cole, YA Gorby, MD Humphrey, JD Istok, FA Spane, JE Szecsody, SS Teel, VR Vermeul, MD Williams, and SB Yabusaki. 1996. *In Situ Redox Manipulation Field Injection Test Report - Hanford 100-H Area.* PNNL-11372, Pacific Northwest National Laboratory, Richland, Washington.

Fruchter JS, MD Williams, VR Vermeul, CR Cole, and SS Teel. 1997. *Treatability Test Plan for In Situ Redox Manipulation in the 100-HR-3 Operable Unit-D Area.* Pacific Northwest National Laboratory, Richland, Washington.

Garrels RM and CL Christ. 1965. *Solutions, Minerals, and Equilibria.* Freeman, Cooper, and Company, San Francisco, p. 450.

Hindmarsh AC. 1983. "A Systemized Collection of ODE Solvers." *Scientific Computing,* RS Stepleman, ed. North-Holland, Amsterdam, pp. 55-64.

IAEA (International Atomic Energy Agency). 1980. *Significance of Mineralogy in the Development of Flowsheets for Processing Uranium Ores.* Technical Reports Series No.196, *International* Atomic Energy Agency, Vienna.

IAEA (International Atomic Energy Agency). 1993. *Uranium Extraction Technology.* Technical Reports *Series* No.359, International Atomic Energy Agency, Vienna.

Kaplan DI and RJ Serne. 1995. *Distribution Coefficient Values Describing Iodine, Neptunium, Selenium, Technetium, and Uranium Sorption to Hanford Sediments.* PNL-10379, Pacific Northwest Laboratory, Richland, Washington.

Langmuir DL. 1978. "Uranium Solution-Mineral Equilibria at Low Temperatures with Applications to Sedimentary Ore Deposits." *Geochimica et Cosmochimica Acta,* 42:547-569.

Maynard JB. 1983. *Geochemistry of Sedimentary Ore Deposits.* Springer-Verlag, New York.

Parker J and MT van Genuchten. 1984. *Determining Transport Parameters from Laboratory and Field Tracer Experiments.* Virginia Agricultural Experiment Station Bulletin 84-3, p. 94.

Payne TE, JA Davis, and TD Waite. 1994. "Uranium retention by weathered schists - the role of iron minerals." *Radiochim. Acta* , 55/56, 301-307.

Pearson RL and ME Wadsworth. 1958. "A Kinetic Study of the Dissolution of UO_2 in Carbonate Solution." *Transactions of the Metallurgical Society of AIME,* Vol. 212, p. 294-300.

Rai D, AR Felmy, and JL Ryan. 1990. "Uranium(IV) Hydrolysis Constants and Solubility Product of $UO_2.xH_2O$ (am)." *Inorganic Chemistry,* 29:260-264.

Salvage KM, GT Yeh, JE Szecsody, and JM Zachara. 1995. "Simulation of $Co^{II/III}EDTA$ Transport at Variable pH Using Two Reactive Transport Numerical Codes." *EOS,* 76: 221, American Geophysical Union, Annual Fall Meeting.

Serne RJ, JL Conca, VL LeGore, KJ Cantrell, CW Lindenmeier, JA Campbell, JE Amonette, and MI Wood. 1993. *Solid-Waste Leach Characteristics and Contaminant-Sediment Interactions. Volume 1: Batch Leach and Adsorption Tests and Sediment Characterization*. PNL-8889 Vol 1, Pacific Northwest Laboratory, Richland, Washington.

Stumm W and J Morgan. 1981. *Aquatic Chemistry*. J. Wiley and Sons, New York.

Szecsody JE, MD Williams, DE Fedele, and JS Fruchter. 1998a. "Use of Dithionite Injection for In Situ Iron Reduction of Sediment for Subsurface Remediation: Chemical Mechanisms During the Redox Cycle." *Environ. Sci. Tech.*, in preparation.

Szecsody JE, JM Zachara, A Chilakapati, PM Jardine, and AS Ferrency. 1998b. "Importance of Flow and Particle-Scale Heterogeneity on Co(II/III)EDTA Reactive Transport." *J. Hydrol.*, in press.

Szecsody JE, JM Zachara, and PL Bruckhart. 1994. "Adsorption-Dissolution Reactions Affecting the Distribution and Stability of Co(II)EDTA in Iron Oxide-Coated Sand." *Environ. Sci. Technol.*, 28: 1706-1716.

Turner GD, JM Zachara, JP McKinley, and SC Smith. 1996. "Surface-Charge Properties and UO+ Adsorption of a Subsurface Smectite." *Geochimica Cosmochimica Acta*, 60:3399-3414.

Waite TD, JA Davis, TE Payne, GA Waychunas, and N Xu. 1994. "Uranium(VI) Adsorption to Ferrihydrite: Application of a Surface Complexation Model." *Geochimica Cosmochimica Acta*, 58:5465-5478.

Wanner H and I Forest (eds.). 1992. *Chemical Thermodynamics Series, Volume 1: Chemical Thermodynamics of Uranium*. North-Holland, Elsevier Science Publishing Company Inc., New York.

Yeh G, G Iskra, JM Zachara, and JE Szecsody. 1998. "Development and Verifications of a Mixed Chemical Kinetic and Equilibrium Model." *Advances in Environmental Research*, 2(1):24-56.

Appendix

Uranium Analysis

Appendix

Uranium Analysis

Uranium concentrations [UO_2^{2+}, U(VI)] were determined using a kinetic phosphorescence analysis (KPA) technique (Brina and Miller 1992, 1993). This technique of measuring the phosphorescence of a uranium complex is accurate to sub-part per billion (µg/L) concentrations. A 0.5-mW pulsed-nitrogen pumped Stilbene-420 dye laser was employed to excite the sample; a 425–nm excitation filter is used between sample cuvette and photomultiplier/photon counter #1. A uranium-based reference solution was used with 100 µg/L U in 0.01 N nitric acid/Uraplex in reference cuvette. A 515 emission filter is used between reference cuvette and photomultiplier/photon counter #2. Excitation of sample is set to 1000 laser pulses of 3 nanosecond duration, with 20 pulses/sec. Luminescence measurements were taken at fixed time intervals (time gates) after the excitation. For uranium, a time-gate duration of 13 microseconds (µs) was selected. The lifetime is the time required for the intensity to fall to 1/e of its original value. A uranium complexant, Uraplex (Chemchek Instruments, Inc. 1995), is mixed with the sample (1:1) to increase the lifetime of the phosphorescence decay prior to excitation.

The first-order kinetic decay equation (A.1) describes the principle of kinetic phosphorescence analysis:

$$\ln [X_t] = \ln [X_0] - (k_p + k_q)t \qquad (A.1)$$

where X_t, X_0 = the population of excited ions at time t (or t = 0), k_p = the rate constant for phosphorescence decay, k_q= the rate constant for nonradiative processes, and t = time in microseconds. The intensity (number of photons) of the phosphorescence signal (I) is proportional to the concentration of the emitting ions, thus

$$\ln [I_t] = \ln [I_o] - (k_p + k_q)t \qquad (A.2)$$

which indicates that the number of detected photons at a given time is directly proportional to the concentration of the excited ions. If a plot of ln $[I_t]$ versus t is generated, the lifetime τ can be calculated from the slope (τ = -1/slope), while the intercept gives ln $[I_o]$, where I_o is the luminescence intensity at the onset of the decay (t = 0). I_o is directly proportional to the concentration of the phosphorus and is independent of quenching effects.

The uranium analyzer (KPA) was calibrated between 0.1 and 150 µg/L uranium from dilutions made from Uranium Standard Reference Material 3164 lot 791402, National Institute of Standards & Technology (NIST), Dept. of Commerce, USA. A 5 µg/L standard dilution was made in 0.1 mol L^{-1} nitric acid. Further dilutions between 0.1 and 150 µg/L U were made in deionized water. Aqueous samples from batch and column experiments were filtered with a 0.1–micron Millex -VV filter unit inside an anaerobic chamber. Filtrates were sealed in 5-mL Falcon polystyrene tubes with Parafilm before being transferred to KPA on the laboratory bench top. The KPA is equipped with a sample changer and a syringe injector for automated injections. Typical instrument error for U analysis, including autodiluting errors, is ±3%.

References

Brina R and AG Miller. 1992. "Direct Detection of Trace Levels of Uranium by Laser-Induced Kinetic Phosphorimetry." *Analytical Chemistry*, 64 (13):1413-1418.

Brina R and AG Miller. 1993. "Determination of Uranium and Lanthanides in Real-World Samples by Kinetic Phosphorescence Analysis." *Spectroscopy*, 8:1-14.

Chemchek Instrument, Inc. 1995. *Operations Manual: Kinetic Phosphorescence Analyzer KPA–11*. Chemchek Instrument, Inc., Richland, Washington.

Distribution

No. of Copies

Offsite

2 Office of Scientific and Technical Information

Grover Chamberlain, EM-54
U.S. Department of Energy
Office of Science and Technology
Cloverleaf Building
2400 Century Blvd.
Germantown, MD 20874

Dr. Randal J. Charbeneau
Pickle Research Campus #119
University of Texas
Austin, TX 78712

Tom Engle, HAB
Department of Civil Engineering
University of Washington
Seattle, WA 98185

Dr. Joseph P. Gould
Georgia Institute of Technology
School of Civil and Environmental Engineering
790 Atlantic Drive
Atlanta, GA 30332

Barbara Harper
Yakama Indian Nation
P.O. Box 151
Toppenish, WA 98984

Stuart Harris
Confederated Tribes of the Umatilla Indian Reservation
P.O. Box 638
Pendleton, OR 97801

No. of Copies

Dr. Alan Moghissi
Institute for Regulatory Science
5457 Twin Knolls Road Ste 312
Columbia, MD 21045

Donna L. Powaukee
Nez Perce Tribe
ERWM Manager
P.O. Box 365
Lapwai, ID 83540-0365

Dr. Vernon C Rogers
Rogers and Associates
P.O. Box 330
Salt Lake City, UT 84110-0330

Philip Washer, DOE-SR
U.S. Department of Energy
Savannah River Operations Office
RFD #1, Bldg. 703A, Rm E208 North
P.O. Box A
Aiken, SC 29802

James A. Wright, DOE-SR
U.S. Department of Energy
Savannah River Operations Office
RFD #1, Bldg. 703A, Rm E208 North
P.O. Box A
Aiken, SC 29802

Onsite

7 DOE Richland Operations Office

D.L. Biancosino	K8-50
J.P. Hanson	K8-50
R.M. Rosselli	K8-50

No. of Copies

	K.M. Thompson	H0-12
	A.C. Tortoso	H0-12
	F.R. Serier	H0-12
	J.P. Neath	K8-50
5	PHMC Team	
	G.C. Henckel	H0-09
	M.A. Buckmaster	H0-19
	J.G. April	H0-05
	M.J. Graham	H0-21
	V.J. Rohay	H9-02
3	U.S. EPA	
	D.A. Faulk	B5-01
	L.E. Gadbois	B5-01
	D.R. Sherwood	B5-01
3	Washington State Department of Ecology	
	D.N. Goswami	B5-18
	W.W. Soper	B5-18
	N.H. Uziemblo	B5-18
1	Washington Department of Fish and Wildlife	
	J.L. McConnaughey	B5-18

No. of Copies

44	Pacific Northwest National Laboratory	
	C.C Ainsworth	K3-61
	S.Q. Bennett	K7-90
	C.L. Blair	K9-14
	W.F. Bonner	K9-14
	K.J. Cantrell (2)	K6-81
	C.R. Cole	K9-36
	J.L. Devary	K6-96
	R.M. Ecker	K6-91
	J.S. Fruchter (10)	K6-96
	K.M. Krupka	K6-81
	W.J. Martin	K9-14
	J.P. McKinley	K3-61
	E.M. Pierce	K6-96
	C.T. Resch	K3-61
	R.J. Serne	K6-81
	J.E. Szecsody (10)	K3-61
	V.R. Vermeul	K6-96
	R.E. Wildung	P7-54
	M.D. Williams	K9-36
	J.M. Zachara	K8-96
	Information Release (5)	K1-06